Experimental data and boundary conditions for a Double - Skin Facade building in preheating mode

Larsen, Olena Kalyanova; Heiselberg, Per; Jensen, Rasmus Lund

Publication date:
2014

Document Version
Publisher's PDF, also known as Version of record

Experimental data and boundary conditions for a Double-Skin Facade building in preheating mode

Olena Kalyanova Larsen
Per Heiselberg
Rasmus Lund Jensen

ISSN 1901-7278
DCE Technical Memorandum No. 40

DEPARTMENT OF CIVIL ENGINEERING
AALBORG UNIVERSITY

Aalborg University
Department of Civil Engineering
Division of Architectural Engineering

DCE Technical Memorandum No. 40

Experimental data and boundary conditions for a Double-Skin Facade building in preheating mode

by

Olena Kalyanova Larsen
Per Heiselberg
Rasmus Lund Jensen

January 2014

Scientific Publications at the Department of Civil Engineering

Technical Reports are published for timely dissemination of research results and scientific work carried out at the Department of Civil Engineering (DCE) at Aalborg University. This medium allows publication of more detailed explanations and results than typically allowed in scientific journals.

Technical Memoranda are produced to enable the preliminary dissemination of scientific work by the personnel of the DCE where such release is deemed to be appropriate. Documents of this kind may be incomplete or temporary versions of papers—or part of continuing work. This should be kept in mind when references are given to publications of this kind.

Contract Reports are produced to report scientific work carried out under contract. Publications of this kind contain confidential matter and are reserved for the sponsors and the DCE. Therefore, Contract Reports are generally not available for public circulation.

Lecture Notes contain material produced by the lecturers at the DCE for educational purposes. This may be scientific notes, lecture books, example problems or manuals for laboratory work, or computer programs developed at the DCE.

Theses are monograms or collections of papers published to report the scientific work carried out at the DCE to obtain a degree as either PhD or Doctor of Technology. The thesis is publicly available after the defence of the degree.

Latest News is published to enable rapid communication of information about scientific work carried out at the DCE. This includes the status of research projects, developments in the laboratories, information about collaborative work and recent research results.

Published 2014 by
Aalborg University
Department of Civil Engineering
Sohngaardsholmsvej 57,
DK-9000 Aalborg, Denmark

Printed in Aalborg at Aalborg University

ISSN 1901-7278
DCE Technical Memorandum No. 40

Recent publications in the DCE Technical Memorandum Series

*** Corresponding author. Tel.: +45 9940 8543; fax: +45 9940 8552. E-mail address: ok@civil.aau.dk**

Abstract

Frequent discussions of double skin façade energy performance have started a dialogue about the methods, models and tools for simulation of double façade systems and reliability of their results. Their reliability will increase with empirical validation of the software. Detailed experimental work was carried out in a full scale test facility 'The Cube', in order to compile three sets of high quality experimental data for validation purposes. The data sets are available for preheating mode, external air curtain mode and transparent insulation mode. The objective of this article is to provide the reader with all information about the experimental data and measurements, necessary to complete an independent empirical validation of any simulation tool. The article includes detailed information about the experimental apparatus, experimental principles and experimental full-scale test facility 'The Cube'. This covers such problem areas as measurements of naturally induced air flow, measurements of air temperature under direct solar radiation exposure, etc. Finally, in order to create a solid foundation for software validation, the uncertainty and limitations in the experimental results are discussed. In part II of this paper the reader will be introduced to the experimental results, and their analysis.

Keywords: Test facility, air flow, tracer gas, velocity profile, air temperature, full-scale measurements

1. Introduction

The Double Skin Facade (DSF) is often being discussed in various scientific publications. This is mainly due to growing interest of the DSF concept among architects because of DSF aesthetical features, sound insulation functions etc.; but there is also an interest among the engineers due to their increasing awareness of the complexity in the design and dimensioning of DSF systems.

Various commercial and free-source building energy simulation programs are used as a powerful tool for the design and evaluation of energy efficiency of buildings and building systems. Results from these building simulations play a significant role when performance of building with or without DSF component is evaluated in terms of energy efficiency and indoor environment. Although, there have been many validation studies that have helped to increase confidence in the use of existing design tools for the performance assessment of conventional buildings, their accuracy for prediction of double façade performance has not been tested to the same extent [1].

Until now, the attempts to validate building simulation tools for DSF modelling purposes have been limited, most of them are known as attempts to validate different models using case studies [2-4]. In the literature, these are explained by the absence of experimental data, inconsistent measurements and by poorly described experimental conditions, which do not allow performing accurate validation [5]. Besides that the multifunctionality of DSF systems in the simulation tool, should, preferably, be validated using experimental data from the same origin.

To address the problem of lacking experimental data a wide range of measurements has been carried out in an outdoor, double-skin façade full-scale test facility 'The Cube'.

The experimental test facility and the experimental set-up described in this paper and, finally, the experimental results obtained within the test facility provide a good foundation for empirical validation of thermal building simulation tools for modelling double skin façade buildings. In this work, the measurements of the mass flow rate and air temperatures in the cavity and adjacent zone are supported with detailed information on the input parameters for a building thermal simulation tool. The generally rare experimental data for the DSF-buildings, containing unique results of the mass flow rate measured in a naturally ventilated cavity.

2. Experimental modes

According to the literature, there are many classification schemas exist for describing the DSF performance [6] and [7]. However, focusing on the energy performance and flow path in the double skin façade, following definition of DSF operational modes is used in this article, as illustrated in Figure 1.

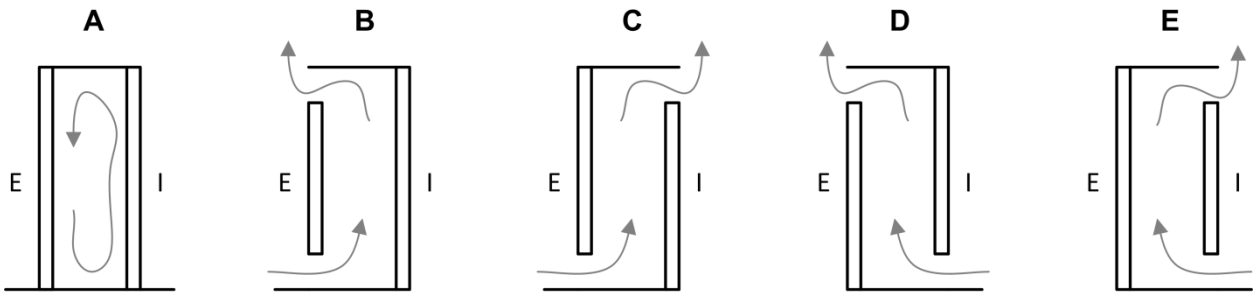

Figure 1. Classification of DSF according to ventilation principle. A- transparent insulation, B-external air curtain, C-preheating mode, D- exhaust mode, E-internal air curtain [7].

Until now, only three ventilation modes were tested, due to time consuming and complex procedure involved with data processing and preparation of experimental set-up. The tested operational modes are present in Table 1.

Operational mode	Experiment duration
External air curtain mode	01.10.2006 – 15.10.2006
Transparent insulation mode	19.10.2006 - 06.11.2006
Preheating mode	09.11.2006 – 30.11.2006

Table 1.Tested operational modes of DSF.

External air curtain mode. The operable windows at the top and bottom of the cavity are open to outside. As a rule, the air enters the DSF at the bottom of the cavity, then it is getting heated while passing through the DSF cavity and released to the external environment, carrying away some amount of the solar heat gains. The flow motion in the cavity is naturally driven and it varies in time.

Transparent insulation mode. All the openings are closed. The principle of this mode is the same as of the conventional window. Air in the DSF cavity is heated to a temperature higher than the outside temperature, this decreases the radiant heat exchange between the internal window surface and the adjacent room.

Preheating mode. In this mode facade openings at the bottom of the cavity are open to the outside and the top openings are open to the interior. The air is preheated in the DSF cavity before entering the room. The air flow is constant and it is driven by the mechanical system in the building.

3. Full-scale test facility

'The Cube' is an outdoor full-scale test facility located near to the main campus of Aalborg University, Denmark. 'The Cube' was built in the fall of 2005, in the frame of IEA ECBCS ANNEX 43/SHC Task 34.

The test facility is designed to be flexible for a choice of the DSF operational modes, natural or mechanical flow conditions, different types of shading devices etc. Moreover, an efficient control of the thermal conditions in the room adjacent to the DSF and the opening control allow to investigate the DSF both as a part of a complete ventilation system and as a separate element of building construction.

'The Cube'(Figure 2) consists of four domains, which are named as: double skin facade, experiment room, instrument room and plant room (Figure 3). The experiment room together with the DSF represents the main building of the test facility, which has external dimensions of 6x6x6 metres. External dimensions of the plant and instrument room together is 6(w)x3x3 metres, which are attached to the northern wall of the experiment room.

Figure 2.'The Cube'. Photo of Southern facade (left) and photo of Northern facade (right).

The key measurements were carried out in the DSF and in the experiment room; meanwhile the instrument room and the plant room were used as a support zone. The instrument room was equipped with dataloggers and computers and the

cooling system was installed in the plant room. In the experiment room, a ventilation system was set up for maintaining uniform conditions in the room.

The temperature in the experiment room was kept constant at approximately 22^{o}C, using a ventilation system with a heating and cooling unit. In order to avoid temperature gradients in the experiment room, a recirculating piston flow with an air speed of approximately 0.2 m/s was used. This resulted in typical temperature gradient of approximately 0.02°C/m and maximum of 0.1°C/m. The air intake for recirculation was at the top of the room. After the intake the air passes through the preconditioning units of the ventilation system and then it was supplied at the bottom of the room through fabric KE-low impulse ducts (Figure 4). Maximum power on cooling and heating units is 10 kW and 2 kW respectively. The weight of ventilation system in the experiment room is approximately 750 kg.

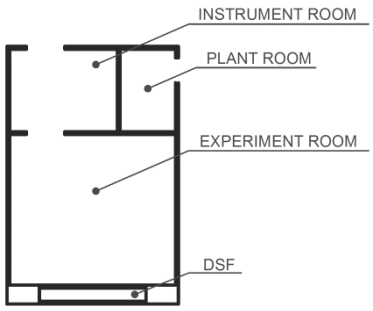

Figure 3. Plan of 'The Cube'.

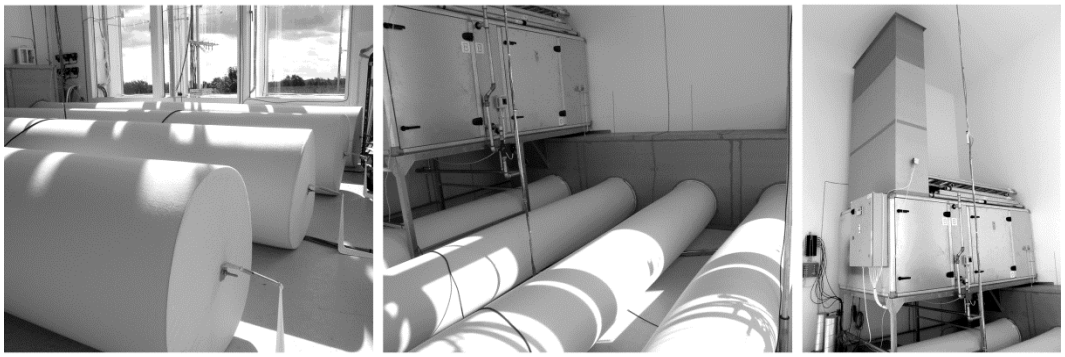

Figure 4. KE-low impulse fabric ducts in experiment room (left, centre). Ventilation system in experiment room (right).

'The Cube' is very well insulated and airtight. The transmission losses of 'The Cube' were determined experimentally. Transmission heat losses were estimated for two set points, when the difference between the air temperature in the experiment room and outdoors was 16 ^{o}C and 21 ^{o}C.

The measurement of overall heat transmission was conducted during a few days with very stable weather conditions, high cloudiness, negligible wind speed and no precipitation. These measurement results (Figure 5) can then be used to adjust the U-values of the constructions to take into account minor thermal bridges in the test facility and any other discrepancies between designed and assembled wall elements.

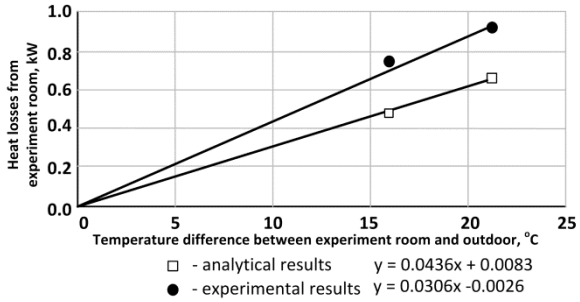

Figure 5. Heat transmission losses of the experiment room.

The air tightness of 'The Cube' was measured during construction, insulation and air tightening of the test facility, before and after installation of experimental set-up to ensure the tightness. The final infiltration rate was 0.2 h^{-1} at 50 Pa of under pressure and 0.35 h^{-1} at 50Pa of overpressure in the experiment room. For that measurement the door to instrument room and plant room were kept wide open, as well as all windows of DSF were fully open.

3.1 Geometry

The exact internal dimensions of the experiment room and double skin façade are summarized in Table 2 and Figure 6.

Zone	Width, mm	Depth, mm	Height, mm	Volumea, m3
DSF	3555	580	5450	11.24a
Experiment room	5168	4959	5584	143.11a

[a]*The volume is calculated to the glass surfaces of the windows and NOT to the window frame*
Table 2. Internal dimensions of DSF and experiment room.

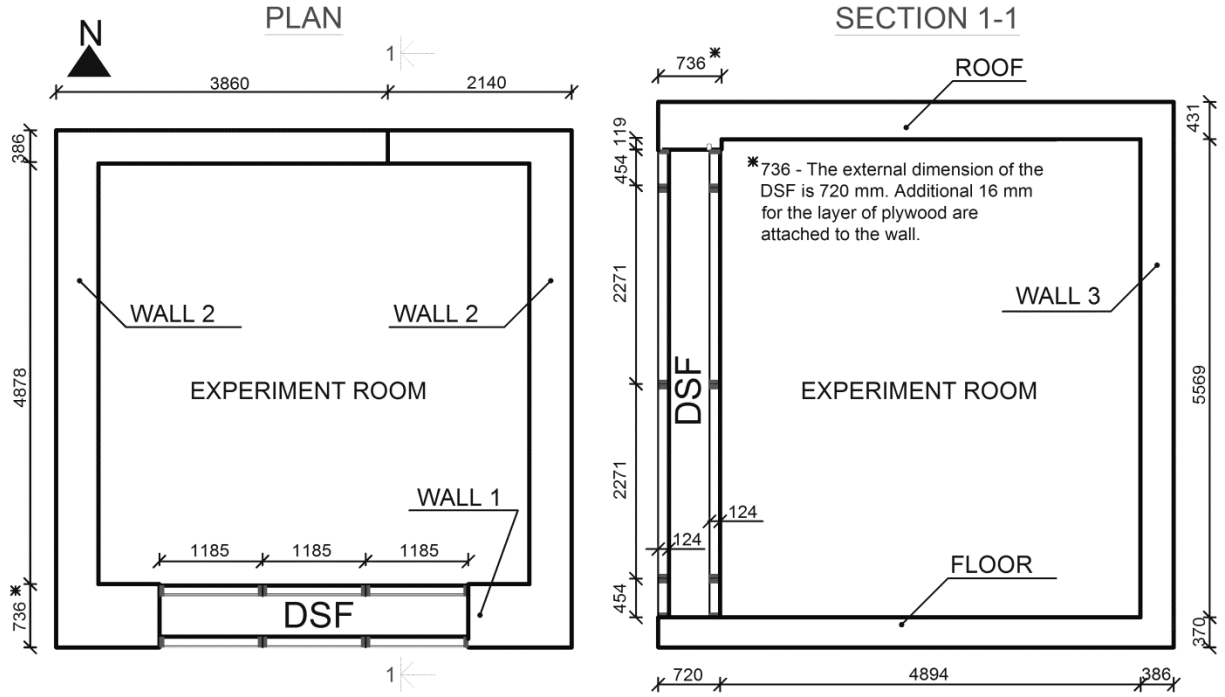

Figure 6. Plan of the experiment room and DSF (left). Section 1-1 of experiment room and DSF (right).

In the Southern façade of 'The Cube' it can be recognized six windows (Figure 2 left). The upper windows have the top operable section and the lower windows have bottom operable section. The dimensions of windows with the top and bottom operable section are identical. Window dimensions are given in Figure 7,
Figure *8* and Table 3.

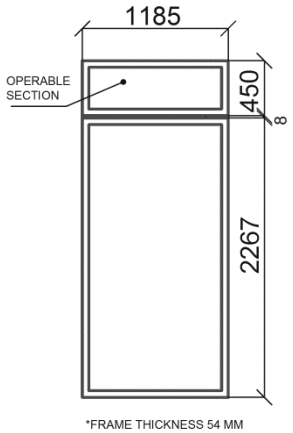

Figure 7. Window dimensions.

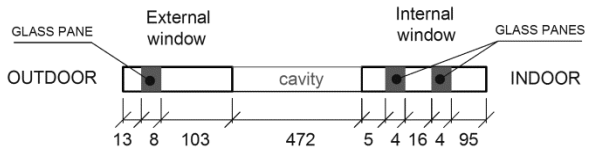

Figure 8.Distances between the glass panes in DSF (distances in mm).

Total area of visible glazing of window, m2	Total frame area of window, m2	Total area of window, m2
2.693	0.536	3.229

Table 3. Glazing and frame areas for the window sections.

3.2 Thermophysical properties of the constructions

Constructions are subdivided into groups, which are:

- Wall 1- the South façade wall, comprise of external and internal windows
- Wall 2- the East and West façade walls
- Wall 3- facing North. A part of this wall is facing the instrument room, another part is facing the plant room, and finally a part of the wall is facing outdoor.
- Roof
- Floor

Thermophysical properties of these constructions are summarised in Table 4. In the table, the first layer always denotes the layer facing the internal environment of the experiment room.

	Layer	Material	Layer thickness, mm	Material density, kg/m3	Thermal conductivity, W/mK	Specific heat capacity, J/kgK	Thermal resistance, m2K/W
Wall 1	1	Plywood	16	544	0.115	1213	0.139
	2	Rockwool M39	620	32	0.039	711	15.897
	3	Isowand Vario	100	142	0.025	500	4
Wall 2	1	Plywood	16	544	0.115	1213	0.139
	2	Rockwool M39	300	32	0.039	711	7.692
	3	Isowand Vario	100	142	0.025	500	4
Wall 3	1	Plywood	16	544	0.115	1213	0.139
	2	Rockwool M39	300	32	0.039	711	7.692
	3	Isowand Vario	100	142	0.025	500	4
Roof	1	Plywood	16	544	0.115	1213	0.139
	2	Rockwool M39	300	32	0.039	711	7.692
	3	Isowand Vario	100	142	0.025	500	4
Floor	1	Reinforced concrete	150	2400	1.800	1000	0.639
	2	Expanded Polystyrene	220	17	0.045	750	4.889

Table 4. Material properties.

3.3 Window properties

External windows of the DSF have one layer of clear glass and the internal windows are low emissivity 4-Ar16-4. Their properties are given in Table 5.

Window	U-value of glazing, W/m^2K	U-value of frame, W/m^2K
External window	5.67	3.63
Internal window partition*	1.12	3.63

** U-values are given for standard conditions, using external-internal surface film coefficients and NOT internal-internal surface film coefficients.*
Table 5. Windows. U-value.

Absorption, reflection and transmission properties of all surfaces in the DSF, experiment room and windows were tested at EMPA Swiss Federal Laboratories for Materials Science and Technology. These are available as a function of the wavelength, in the interval of 250-2500nm. Corresponding properties of window panes are given in Table 6. The emissivity of the glass surfaces is summarized in Table 7.

Incident angle	External window			Internal window			
	Transmission of solar radiation	Reflection of solar radiation	g-value	Transmission of solar radiation	Reflection of solar radiation FRONT	Reflection of solar radiation BACK	g-value
0	0.763	0.076	0.8	0.532	0.252	0.237	0.632
10	0.763	0.076		0.531	0.252	0.237	0.632
20	0.76	0.076		0.529	0.251	0.237	0.631
30	0.753	0.078		0.524	0.252	0.239	0.627
40	0.741	0.084		0.513	0.258	0.245	0.618
50	0.716	0.103		0.488	0.277	0.264	0.595
60	0.663	0.149		0.435	0.326	0.309	0.542
70	0.55	0.259		0.331	0.436	0.405	0.433
80	0.323	0.497		0.163	0.638	0.579	0.244
90	0	1		0	1	1	0

Table 6. Glazing properties.

Window	Front*	Back
External window	0.84	
Internal window, filled with Argon, 90 %	0.84	
	0.037	0.84

** Front side is always turned towards the exterior, while back is turned towards the interior*
Table 7. Emissivity of glazing.

3.4 Openings

The discharge coefficient describes a correlation between the actual and ideal discharge of fluid through an opening and thus it is highly related to the flow rate. The difference between the actual and ideal discharge is caused by the friction forces at the edges of an opening and the jet contraction. In general, the airflow across an opening can be described as in equation (1), meanwhile the discharge coefficient can be calculated as in equation (2).

$$Q_v = \pm C_D \cdot A \cdot \sqrt{\frac{2 \cdot |\Delta P|}{\rho}} \quad (1)$$

$$C_D = \frac{Q_v}{A \cdot \sqrt{\frac{2 \cdot |\Delta P|}{\rho}}} \quad (2)$$

Q_v – is volume flow, [m^3/s]
C_D – is discharge coefficient, [-]
A – is opening area, [m^2]
ρ – is air density, [kg/m^3]
ΔP – is pressure difference across the opening, [Pa]

The discharge coefficients for different opening degrees in the experimental set-up were estimated experimentally by measurement of pressure difference across the opening and by computations as in equation (2). These measurements were performed in a laboratory, maintaining constant flow across the opening in isothermal conditions.

The opening degree of the windows, and corresponding discharge coefficients are given in Table 8. Meanwhile, the definition of the opening angle and dimensions provided in Table 8 are illustrated in Figure 9.

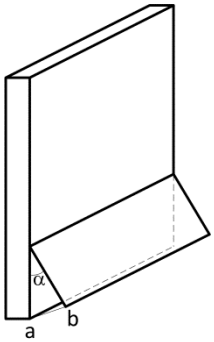

Figure 9. Definition of opening degree for a window.

	Top opening	Bottom opening
External air curtain mode		
Discharge coefficient	0.72	0.65
Distance 'ab', m	0.09	0.110
Angle α, deg	11.5	14
Preheating mode		
Discharge coefficient	0.35	0.65
Distance 'ab', m	0.068	0.068
Angle α, deg	8.5	8.5

Table 8. Opening degree.

Discharge coefficients for the openings are defined assuming that the air enters the cavity at the bottom and leaves at the top (Figure 10). In case of reversed flow, given value of discharge coefficient is not valid, as the friction forces and the jet contraction at the opening will differ from a given scenario.

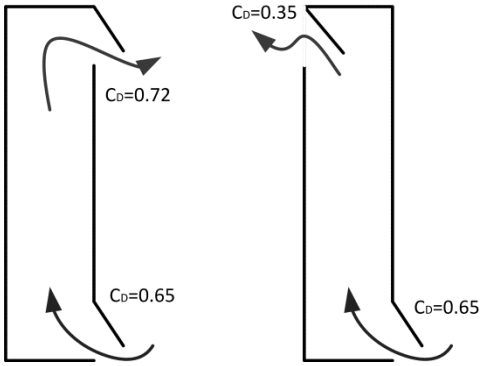

Figure 10. Illustration of openings with corresponding discharge coefficients. External air curtain mode (left), preheating mode (right).

3.5 Surface properties and ground properties

For reliable estimation of ground-reflected solar radiation, a large carpet was placed on the ground in front of the southern façade of 'The Cube' to achieve uniform reflection from the ground. The fabric of the carpet was chosen so that it does not change its reflectance property when it is wet due to its permeability. Reflectance is approximately 0.1, close to the generally assumed ground reflectance. The size of the carpet corresponded to a view factor of 0.5 between the DSF and the ground.

The reflectance property of wall finish in DSF corresponds to 65% and in experiment room it corresponds to 67%, because of different type of painting used.The reflectance property of the floor surface in both of the zones and of the external surfaces is 65%.

3.6 Wind pressure coefficients

The wind pressure coefficients are found from the literature [8], where pressure coefficients were measured for a building of the same dimensions as 'The Cube', see Table 9.

Location	Wind angle to Southern facade							
	0	45	90	135	180	225	270	315
Top openings	0.58	0.22	-0.71	-0.5	-0.36	-0.5	-0.71	0.22
Bottom openings	0.61	0.33	-0.55	-0.5	-0.35	-0.5	-0.55	0.33

Table 9. Wind pressure coefficients.

3.7 Building site

The following coordinates define the geographical location of the building (Table 10):

Time zone	+1 hr MGT
Degrees of longitude	9°59'44.44"E
Degrees of latitude	57° 0'41.30"N
Altitude	19 m

Table 10. Geographical and site parameters for the model.

The wind profile for the local terrain is established from 6 month measurement of wind speed and direction at six different heights above ground. The mathematical model describing the wind profile is obtained on the basis of logarithmical wind profile using the least square method. It is given by equation (3), where *V(h)* is the wind speed at height h, h is the height above ground and V_{10} is the wind speed at height 10 metres above the ground.

$$V(h) = V_{10} \cdot \ln\left(\frac{h}{0.31}\right)/3.47 \qquad (3)$$

3.8 Weather data

Assembled weather data includes wind speed, wind direction, outdoor air temperature, relative humidity, global and diffuse solar radiation, and atmospheric pressure.

The experimental data is available for the test cases in the period from October to December 2006. In Denmark, this period of a year is characterized by a contrast in the day-time and night-time air temperature. Besides, in autumn the day-time outdoor air temperature is relatively low while the solar irradiation stays relatively strong. And finally, the weather conditions and the length of a day in October and December differ a lot. The periods with lack of climate data were replaced by data purchased from Danish Meteorological Institute, measured at Aalborg airport, which is located 12km away from the Cube.

In Table 11 the climatic boundary conditions are divided into three groups, corresponding to each test mode. The table does not include total solar irradiation measured on a vertical surface of DSF, relative humidity and atmospheric pressure, but this data is also available.

MODE		Outdoor air temperature, oC	Wind speed, m/s	Diffuse solar irradiation, W/m2	Total solar irradiation on horizontal, W/m2
Ext. air curtain	MIN	4.3	0.1	0	0
	MEAN	12.5	3.6	91a	175a
	MAX	19.5	14	302	554
	STD	2.8	2.5	64a	143a
Transparent insulation	MIN	-2.6	0	0	0
	MEAN	9.6	5.2	58a	89a
	MAX	17.1	20.8	261	372
	STD	4	3.7	46a	87a
Preheating	MIN	0.4	0.55	0	0
	MEAN	7.5	5.2	36a	51a
	MAX	14.1	12.3	188	341
	STD	2.4	2.3	34a	57a

[a] *Mean and standard deviation for solar irradiation is given only for the periods with sun.*
Table 11. Statistical analysis of climate data for three operational modes.

3.9 Non-climatic boundary conditions

Thermal conditions in the plant room and the instrument room define the boundary conditions in the experiment room. Therefore, the temperature variation in these rooms has to be considered for validation. In Table 12 the average room temperatures for the period of measurements are summarised. The distribution of these room temperatures over the measurement period is also available.

Mode	Instrument room	Plant room
Transparent insulation	18.3	12.3
External air curtain	18.5	14.7
Preheating	18.7	12.1

Table 12. Average air temperature in the rooms.

4. Experimental set-up

All experimental results, including the weather data are available for 1-hour and 10-minutes time interval. The following are the parameters available for validation of building simulation programs:

Primary parameters:

- Solar radiation striking on the external surface of the DSF
- Air temperature in the DSF cavity
- Temperature gradients in the cavity
- Cooling/heating load to experimental room
- Mass flow rate in the DSF cavity

Secondary parameters:

- Surface temperature of the glazing
- Surface temperature of opaque constructions

4.1 Assembling the weather data

Wind velocity and wind direction was measured in six points above the ground, in order to build a vertical wind velocity profile. Both 2D and 3D ultrasonic anemometers were placed on the mast in the centre line of the building, 12m away from its Southern facade.

Outdoor air humidity was measured every 10 minutes, using portable COMARK data logger N2003 from Comark Instruments Inc.

Outdoor air temperature was measured using two thermocouples type K, at the height of 2 m above ground. Both of the thermocouples were silver coated and placed shaded from the direct sun. The measurement took place every 60 seconds.

BF3 pyranometer measured global and diffuse solar irradiation on the horizontal surface. Another pyranometer, Wilhelm Lambrecht, type 1027, measured only Global solar irradiation on the horizontal surface and was placed on the roof for control of BF3-readings. Solar radiation received on the vertical surface of DSF was measured with Wilhelm Lambrecht-pyranometer, type 1550. Readings from pyranometer devices were taken every 60 seconds.

4.2 Temperature measurement

Depending on location of the sensor, temperature was registered with two frequencies: every 0.2 second and every 60 seconds. High frequencies were used for the measurement of air temperature in DSF cavity and the temperatures of exhaust air from the cavity, only.

The air temperature was measured in plant room, instrument room, DSF and experiment room. Also, the ground temperature, underneath of foundation in experiment room was measured.

In [9] and [33] it is explained that the presence of direct solar radiation is an essential element for the facade operation, but it can heavily affect measurements of air temperature and may lead to errors of high magnitude using bare thermocouples and even adopting shielding devices. Taking this into consideration, the thermocouples in DSF cavity were protected from an influence of direct solar radiation by silver coated and ventilated tube, air flow through the tube was ensured by a minifan. Thermocouples were placed in each DSF section in several heights, enough to build a vertical temperature gradient.

The air temperature in the experiment room was measured with bare silver coated thermocouples and a shielded-ventilated thermocouple with silver coating, which were placed at different heights in four locations in the room.

Surface temperature of walls was also measured in experiment room and DSF: thermocouples were glued to surfaces with a paste of high heat transmission property.

Measurement of glazing surface temperature was performed in the centre of glazing pane for each window section. The temperature was measured of:

- internal surface of inner window pane

- external surface of inner window pane
- internal surface of outer window pane

These measurements were conducted with sensors shielded from direct solar access. Continuous shading of the thermocouple sensor at the inner pane was provided by a thin aluminium foil fixed around sensor at the external surface (Figure 11). As a result, the foil shielded both a sensor at the external and internal surfaces. The thermocouple at the internal surface of the outer pane was protected in a similar way by a piece of aluminium sticky tape on the external surface of the outer pane.

Figure 11. Measurement of glass surface temperature. Thermocouples are shielded by silver foil.

4.3 Power supply in the experiment room

One of the main targets of this experimental work was to accurately estimate solar gains to the experiment room adjacent to the double skin facade. Solar gains to the experiment room can be used as a measure of DSF performance and they can be estimated from the heat balance in the room if cooling/heating loads are known.

Cooling load

Water was used in the cooling unit of the ventilation system. With the purpose to avoid condensation on the surface of the cooling unit the minimum water temperature was set to 12 ^{o}C, this resulted in a large area of cooling surface and the size of whole system. The difference between the supply and return water temperature from the cooling unit was measured with thermopile and recorded by Helios data logger at a frequency 0.1 Hz.

In order to avoid measurement errors associated with small mass flow rates of water, a constant water flow rate was used; meanwhile the cooling load to the room was achieved due to variation of the water temperature.

Heating load

The heating unit in the ventilation system was rarely activated, as the running fan of ventilation system in the experiment room ensured an additional heat load. Moreover, some equipment had to be installed in experiment room and resulted in more additional loads. For keeping a track of all loads to experiment room, including the heating unit, all equipment in the room was connected to a wattmeter D5255S from producer Norma. Readings from the wattmeter were assembled at a frequency 0.1 Hz by a data logger Helios.

4.4 Air flow

Assessment of the air change rate is of key importance for the evaluation of a double skin façade performance, at the same time the measurement of naturally induced air flow is known for its complexity.

In the literature, there are a few methods used for estimation of the air change rate in a naturally ventilated space. The most known experimental methods are the tracer gas method, a method of calculating the air flow from the measured velocity profiles in an opening and using a scale modelling [10-12].

Experimental investigation of the air flow rate requires measurement of many highly fluctuating parameters. The fluctuation frequency implies the high sampling frequency for the measurements. For example according to Larsen (2006), the wind speed has to be measured at least at the frequency of 5 Hz, otherwise peaks in the wind velocity can be lost when averaged in time. When measured with the tracer gas method the limitations are extended to the air flow rates, as with the high air flow rate the amount of injected tracer gas will be enormous. Because of these reasons, the investigation of the natural air flow often is carried out in the controlled environment of the wind tunnel or scale models.

Two methods were used for the air flow measurements in ‘The Cube’, these are:

- Velocity profile method

- Tracer gas method

Velocity profile method

This method requires a set of anemometers to measure a velocity profile in the opening, as illustrated in Figure 12, which gives an example for velocity profile measurement in an opening. Meanwhile, possible flow patterns are illustrated in Figure 13, according to [30]. In the method, the shape of the determined velocity profile depends on amount of anemometers installed. Therefore the number of anemometers used for the measurement must be sufficient to provide the minimum necessary resolution of shape of the velocity profile. At the same time, the equipment located directly in the opening can become an obstruction for the flow appearance. Thus, the method becomes a trade off between the maximum desired amount of anemometers and the minimum desired flow obstruction. Instead of placing equipment directly in the opening in the case of the double skin facade, it can be placed in the DSF cavity, where the velocity profile can be measured in a few levels instead of one, for better accuracy.

Figure 12. Measurement of velocity profiles in an opening. View from inside (left), view from outside (right).

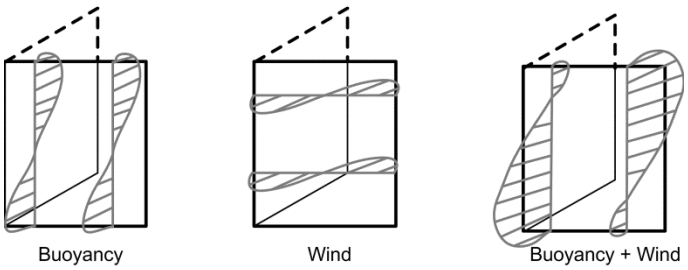

Figure 13. Flow patterns through open windows in single-sided ventilation [13].

For the double skin façade, the negative aspect of this method is explained by air flow variation, as the instantaneous air velocity in the cavity may vary from 0 to 5 m/s. This velocity range is challenging, as the equipment must be suitable for measurements of both low and higher velocities. Moreover it is necessary to be able to follow the flow fluctuations. As explained earlier by Jensen [14] the hot-sphere anemometers have proved to be suitable for the task. These were also tested for uncertainties when measure under the direct solar radiation.

During experiments in ‘The Cube’ all of the velocity measurements were conducted in the central section of DSF, the velocity profiles were measured in 6 levels, with various number of anemometers at different levels. Levels are numbered with the Roman numbers in the Figure 14. All in all 34 hot-sphere anemometers were installed in the experimental set-up. 24 hot-sphere anemometers had measurement frequency of was 10 Hz, the other 10 anemometers had a measurement frequency of 0.2 Hz and were located in level I and level II (Figure 14).

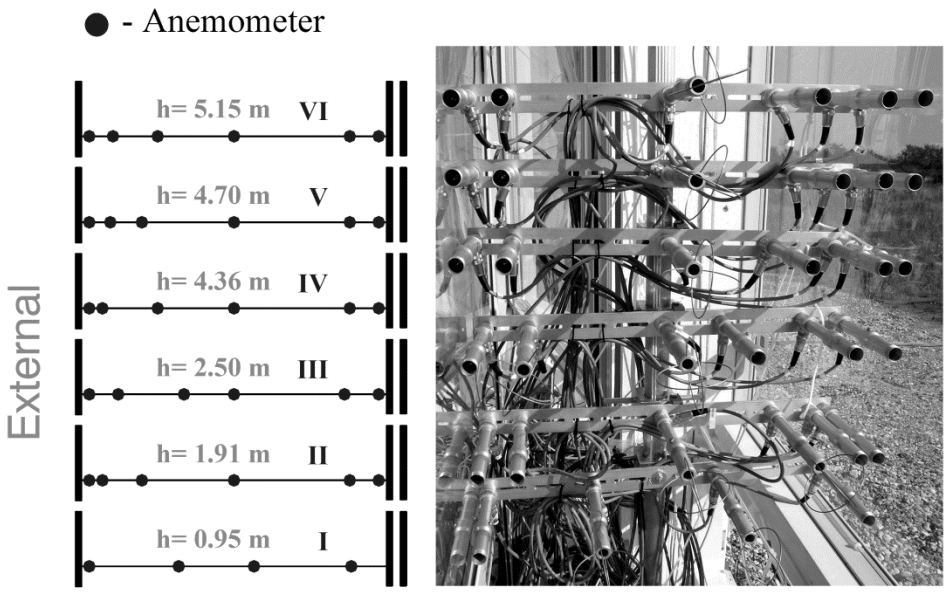

Figure 14. Positioning of anemometers in the DSF cavity (left). Anemometers in the DSF cavity before they were moved up to their respective heights (right).

Tracer gas method

The measurements were completed with the constant injection method. In this method, the tracer gas is injected at a constant rate and then the concentration response is recorded [12]. According to McWilliams [15] the constant injection method is more appropriate for leaky spaces where the gas would be quickly ventilated from the space, thus it is suitable for DSF. However, according to [12] and [15] this method is not appropriate for highly unsteady ventilation rates i.e. in a naturally ventilated DSF cavity. Thus the measurement accuracy may suffer.

Carbon dioxide (CO_2) is the tracer gas used during the whole period of experiments. Carbon dioxide was released in the lower part of the double skin facade cavity, but above the bottom openings. Even distribution of the tracer gas along DSF cavity was ensured by its injection through a perforated tube of internal diameter 3.5 mm, perforation distance 4 mm and 0.5 mm diameter of perforations. Samples of the tracer gas dilution were taken in 12 points (4 samples per section) at the top of the DSF cavity, but below the top openings, Figure 15. All samples were blended together in collector and then the concentration of the diluted tracer gas was measured by a gas analyzer BINOS.

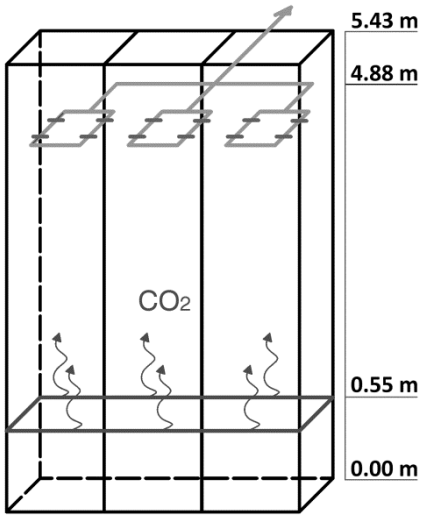

Figure 15. Experimental set-up for the tracer gas method: positioning of the perforated tube for the release of the tracer gas at the bottom of DSF cavity and the air intakes for polluted air, at the top of DSF cavity.

Concentration of carbon dioxide in the outdoor (incoming) air was measured continuously, by a gas analyzer URAS. The Helios data logger collected the measurement data from the gas analyzers with the frequency 0.1 Hz. The constant injection method was used during the experiments and quantity of released tracer gas was kept constant (apx. 4 l/min).

5. Accuracy and uncertainty of experimental data

Assessment of measurement accuracy is crucial for empirical validation. Here the uncertainties related to the experimental methods are discussed and the accuracy of the instruments is reported. Prior to the measurements, the accuracy of all measurement equipment was checked. All of the instruments and sensors were calibrated for the suitable measurement conditions to reduce measurement uncertainty. The measurement uncertainty is summarised in Table 13.

Temperature HELIOS datalogger HBM datalogger	 +/- 0.07 ^{o}C +/- 0.14 ^{o}C
Solar radiation Diffuse on horizontal surface Total on horizontal surface Total on vertical surface (DSF)	 +/- 10 % +/- 2% +/- 3%
Wind speed 3D ultrasonic anemometers 2D anemometers	 +/- 1% +/- 4%
Wind direction 3D ultrasonic anemometers 2D anemometers	 +/- 3^{o} +/- 3^{o}
Cooling/Heating Load Supply and return water temperature Water mass flow rate Wattmeter	 +/- 0.07^{o}C +/- 0.1% +/- 0.1 %
Air velocities Hot sphere anemometers	 +/- 0.05 m/s
Concentration of CO2 In the DSF (BINOS) In the outdoor air (URAS)	 +/- 10 ppm +/- 10 ppm

Table 13. Measurement uncertainty of equipment used in the experimental set-up.

In the experimental studies, there are four experimental methods deserving special attention for uncertainty considerations. These are:

- Tracer gas method with constant injection of CO_2 for assessment of the air change rate in the DSF cavity
- Velocity profile method for assessment of the air change rate in the DSF cavity
- Measurement of air temperature under direct solar radiation
- Measurement of air velocity with the hot sphere anemometers exposed to direct solar radiation

Tracer gas method with constant injection of CO_2. This method requires the minimum amount of measurements and equipment, but it is characterized with frequent difficulties to obtain uniform concentration of the tracer gas, disturbances from wind and the time delay of the signal caused by the time constant of the gas analyzer.

According to McWilliams [32], tracer gas theory assumes that tracer gas concentration is constant throughout the measured zone. For the tracer gas method an error in determined air flow is expected in the range of 5-10 %, which requires full mixing of the tracer gas and air in the DSF cavity.

In the tracer gas method, the main errors appear when the tracer gas is not well mixed with the entrance air, or when there are wind wash-out effects, reversed flow and/or recirculation flow. With wind washout or flow reversal the tracer gas is removed from the DSF cavity: in practice this is indicated by very high readings of the air flow rate.

Both the wind washout effect and the reversed flow appear due to highly fluctuating wind. Yet a particular and noteworthy difference between these two phenomena is the fluctuating parameter of wind: the fluctuating wind speed in case of reversed flow phenomenon and the fluctuating wind direction in case of wind washout effect.

The wind washout effect is explained as an additional flow pattern that occurs in the DSF cavity, taking place in the horizontal plane. The wind washouts appear due to different wind pressure distribution at the openings in the same façade and at the same height. These differences in the pressure distribution appear primarily due to wind direction. In Figure 16, two different scenarios for wind pressure distribution on a façade are illustrated. In the figure the illustration to the right is visualizing the effect of wind direction, meanwhile the illustration to the left is focused on effect of the wind speed for the reversed flow. In case of reversed flow, the buoyancy forces are significantly weaker than the wind pressure at the top openings of DSF. Correspondingly the reversed flow phenomenon is characterized by fluctuations in the wind speed compared to magnitude of buoyancy.

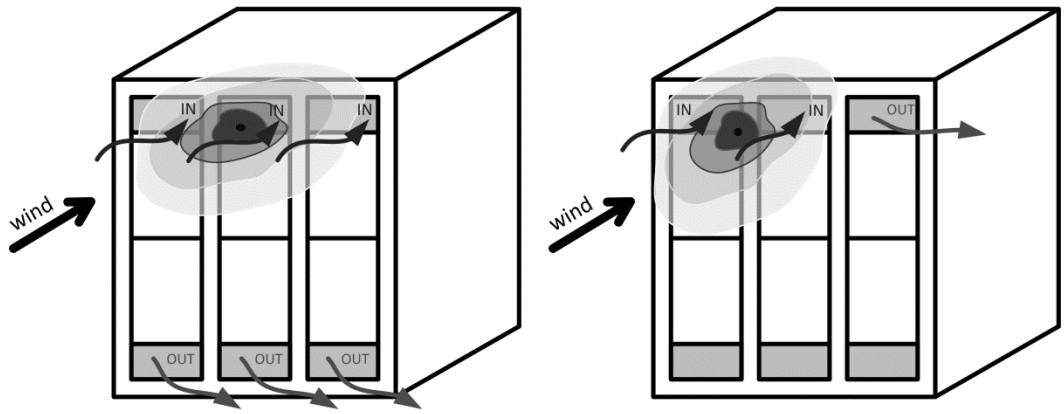

Figure 16. Illustration of reverse flow (left) and wind washout (right) for DSF.

From the measurements, it was observed that the appearance of reverse flow is periodical (with weak buoyant forces, where the wind pressure at the top of the DSF is greater than that at the bottom). The wind washout effect is a similar phenomenon to reverse flow, but its occurrence is more random and originates from the highly fluctuating wind.

It is not possible to quantify the impact of poor mixing. The flow regime in the DSF cavity is turbulent and highly fluctuating; therefore, good mixing of air and tracer gas was expected, except when disturbed by wind washouts or flow reversal, causing removal of tracer gas from the cavity.

Velocity profile method. The velocity profiles are measured only in the central section in the cavity. Accordingly, one of the significant limitations in this method is the assumption of equal flow conditions in all three sections of the DSF cavity, which is not necessarily true in practice.

This method is also sensitive to the number of velocity sensors and their location in the plane, as poor approximation of the velocity profile will result in inferior accuracy. For better estimation of the velocity profile, knowledge of the flow conditions and flow patterns is needed.

Another limitation related to this method is the boundary layer flow, which can result in overestimation of the air flow rate in the cavity, both on days with strong solar radiation or at night. Accordingly, in the periods when the boundary flow at the surfaces of the DSF cavity is relatively strong, overestimation of mass flow rate will take place.

Measurement of air temperature and air velocity under direct solar radiation

Measurement accuracy can suffer significantly if sensor, measurement device or data acquisition system is exposed to a strong direct solar radiation. This is particularly important for the accuracy of temperature measurements or measurement principles which involve temperature compensation. For the described experimental set-up in ‘The Cube’, measurement of air velocity using a hot-sphere anemometers and air temperature measurements are distinguished as the most sensitive to solar radiation exposure.

In [16] different shielding techniques are investigated for protection of temperature sensors for accurate measurement of air temperature under the solar radiation exposure. It is concluded that silver coating of the sensor together with silver coated ventilated tube is the sufficient way for sensor protection, which minimizes the uncertainty in temperature measurement caused by presence of solar radiation.

On contrary to thermocouples which need protection, the hot sphere anemometer measurements stay unaffected by solar radiation as explained in [14].

Besides the above mentioned measurement methods, it is also necessary to mention limitations associated with the test facility. The most significant limitations were caused by the need to maintain constant air temperature in the experiment room. It was achieved by installing ventilation system in the room together with the KE-low impulse fabric ducts. This resulted in following limitations:

1. Ventilation system of 750 kg weight placed in the experiment room serves an additional thermal mass in the room, and therefore affects the distribution of cooling/heating loads during the period of experiments.
2. Piston flow in the room can significantly affect convective heat transfer in the room, this limitation, however, is disregarded due to rather low air speed (max 0.2 m/s).
3. Positioning of fabric ducts on the concrete floor of experiment room can cause two problems. The first problem is explained by discrepancies in absorbtion of solar radiation by the floor construction with and without fabric ducts. Another problem is that the temperature of the air that is supplied through the fabric ducts is normally different from the room air temperature (the supply temperature is normally cooler during the peak solar loads). As a result, the concrete floor serves as a thermal mass, which is cooled down or heated up, depending on the supply air temperature.

The above mentioned limitations of the experimental set-up have to be taken into consideration when using the experimental data for software validation, by adjusting the model to suite the experimental conditions.

7. Summary

Good quality data sets were compiled for three operational modes of the double skin façade. These are external air curtain mode, transparent insulation mode and preheating mode. Each set of data is complete and can be valuable for empirical validation of building simulation software or other research purposes.

Although, all described measurement methods have sources of error and compared to laboratory conditions have relatively large uncertainties, their results has shown reasonable agreement and can be used for experimental validation of numerical models for double facade.

Finally, this experimental data set has several advantages over already existing DSF monitoring results, which include:

- The data set contains long term measurements of naturally induced air flow in a cavity from non-laboratory conditions.
- The data sets are prepared for a period of approximately two weeks, meanwhile published results are only available for significantly shorter periods. Certainly, there are publications with longer measurement intervals available, but those are characterized with very limited number of parameters that have been measured.
- Three functioning modes of DSF are tested in the same façade system, using the same measurement principles and equipment. Moreover, these were carried out by the same team, which means that if there are any personal judgment errors present, than these are consequent for the whole set of experiments.
- And, finally, the data set is composed from monitoring results in the full-scale test cell, which is on contrary to laboratory conditions, does not require duplication of 'real climate' effects [17]. Also, opposite to real building monitoring, full-scale test cell is designed, insulated, air tightened entirely for the measurement purposes. As a result, its geometry, thermophysical properties of the constructions and boundary conditions are well documented; the measurements are performed in well controlled conditions, using calibrated instruments and sophisticated acquisition systems.

Acknowledgement

This work has been conducted in the framework of IEA SHC Task 34 /ECBCS Annex 43 "Testing and Validation of Building Energy Simulation Tools" and it was supported by the Danish Technical Research Council.

Note

All experimental data, including boundary conditions for the described operational modes are attached as appendix.

In case of questions or discovered errors, please contact the corresponding author ok@civil.aau.dk

References

[1] O. Kalyanova, P. Heiselberg, C. Felsmann, H. Poirazis, P. Strachan, A. Wijsman, An Empirical Validation of Building Simulation Software for Modelling of Double-Skin Facade (DSF), IBPSA 11. (2009).

[2] J. von Grabe, A prediction tool for the temperature field of double facades, Energy Build. 34 (2002) 891-899.

[3] L. Mei, D. Infield, U. Eicker, V. Fux, Thermal modelling of a building with an integrated ventilated PV façade, Energy Build. 35 (2003) 605-617.

[4] Y. Takemasa, M. Hiraoka, M. Katoh, H. Tsukamoto, M. Tanabe, H. Tanaka, Performance of Hybrid Ventilation System Using Double-Skin Facade and Vertical Airshaft, 52 (2004).

[5] K. Gertis, A critical review of Double Glazing Facades Under Aspects of Building Physics, German Journal Bauphysik. 21 (1999) 54-66.

[6] H. Poirazis, Double Skin Facades. A Literature Review, (2006).

[7] X. Loncour, A. Deneyer, M. Blasco, G. Flamant, P. Wouters, Ventilated Double Facades - Classification & Illustration of Facade Concepts, (2004) 49.

[8] M.P. Straw, Computation and measurement of wind induced ventilation, PhD Thesis, School of Civil Engineering, The University of Nottingham, UK. (2000).

[9] O. Kalyanova, P. Heiselberg, Final Empirical Test Case Specification. Test Case DSF100_e and DSF200_e. DCE Technical Report 33 (2008).

[10] T. Larsen, P. Heiselberg, Single-sided natural ventilation driven by wind pressure and temperature difference, Energy Build. 40 (2008) 1031-1040.

[11] E.R. Hitchin, C.B. Wilson, A review of experimental techniques for the investigation of natural ventilation in buildings, Building Sciences. 2 (1967) 59-82.

[12] D. Etheridge, M. Sandberg, Building ventilation: theory and measurement (1996) 724.

[13] W. De Gids, H. Phaff, Ventilation rates and energy consumption due to open windows: a brief overview of research in the Netherlands, Air Infiltration Review. 4 (1982) 4-5.

[14] R. Jensen, O. Kalyanova, C. Hyldgaard, On the use of hot-sphere anemometers in a highly transient flow in a double-skin facade, Roomvent. (2007).

[15] J. McWilliams, Review of air flow measurement techniques, (2002).

[16] O. Kalyanova, F. Zanghirella, P. Heiselberg, M. Perino, Measuring Air Temperature in Glazed Ventilated Facades in the Presence of Direct Solar Radiation, Roomvent. (2007).

[17] P. Strachan, Model validation using the PASSYS Test cells, Build.Environ. 28 (1993) 153-165.

ISSN 1901-7278
DCE Technical Memorandum No. 40